

observed for simple adsorption onto the reduced metal surface (compare Figures 4c and 6a).

The change in the kinetics of adsorption are strong evidence for the proposed model. Indeed, in no previous study has there been a shift from slow to rapid kinetics until physical adsorption began to dominate. The observed acceleration in the adsorption process at the same point at which there was a virtual step change in the heat of adsorption strongly suggests that there was a fundamental shift in the surface process. This raises a second question: Why doesn't the simple hydrogen adsorption process begin until all of the surface has been reduced? The answer is that the titration process is a true equilibrium process, such that all available hydrogen will rapidly diffuse on the particle surfaces until it reduces any remaining oxygen. Only following the removal of all of the oxygen will the heat of simple hydrogen adsorption not be masked. Indeed, this model is in agreement with the gradual decrease in rate observed in the first stage of the process. The hydrogen must first adsorb and then diffuse to the site of oxygen atoms. The slowing rate of this reduction process suggests that the reduction process requires progressively larger activation energy.

Summary

A thorough calorimetric investigation of graphite-supported iridium particle chemistry was conducted. A careful determination of the particle size distribution assisted in the interpretation. The stoichiometry of oxygen, carbon monoxide, and hydrogen was determined: $\text{CO}/\text{Ir}_s = 0.50$, $\text{O}/\text{Ir}_s = 1.0$, $\text{H}/\text{Ir}_s = 1.0$. The

differential heats of adsorption of these molecules on the iridium surface was found to be very similar to those reported for alumina-supported iridium particles, suggesting support effects are minimal. Differential rate data were made available for the first time. It is clear that this basic information regarding adsorption stoichiometries, rates, and heats will be useful in future studies of the surface composition of multimetallic supported catalysts that contain iridium.

The calorimeter allowed a study of the interaction between hydrogen and oxygen on an iridium surface. The rate, heat, stoichiometry, and sequence of steps that occur when differential hydrogen reduction of a preoxidized surface is carried out were all studied. It was found that the heat of reaction and the rate of reaction between dosed hydrogen and adsorbed oxygen progressively decreased. The measured integral heat, however, agreed with a simple thermodynamic model. The results of this study suggests that differential calorimeters can be valuable tools for providing information of the type required for detailed kinetic modeling of reactions taking place on catalyst surfaces. They also suggest that this type of calorimetry can provide detailed insight into the mechanism of surface reaction, an area of intense research at the present time.

Acknowledgment. We are grateful to the National Science Foundation (Grant No. CTS 8915 194) for providing financial support for this work.

Registry No. O_2 , 7782-44-7; H_2 , 1333-74-0; Ir, 7439-88-5; CO, 630-08-0; graphite, 7782-42-5.

A Raman and Ultraviolet Diffuse Reflectance Spectroscopic Investigation of Silica-Supported Molybdenum Oxide

Clark C. Williams,[†] John G. Ekerdt,*

Department of Chemical Engineering, University of Texas at Austin, Austin, Texas 78712

Jih-Mirn Jehng, Franklin D. Hardcastle,[‡] Andrzej M. Turek, and Israel E. Wachs

Zettlemoyer Center for Surface Studies, Departments of Chemical Engineering and Chemistry, Lehigh University, Bethlehem, Pennsylvania 18015 (Received: September 4, 1990; In Final Form: May 29, 1991)

Laser Raman spectroscopy (LRS) and ultraviolet-visible diffuse reflectance spectroscopy (UVDRS) were used to characterize silica-supported, hydrated molybdenum oxide prepared from $(\text{NH}_4)_6\text{Mo}_7\text{O}_{24}\cdot 4\text{H}_2\text{O}$, $\text{H}_2(\text{MoO}_3\text{C}_2\text{O}_4)\cdot 2\text{H}_2\text{O}$, MoCl_5 , $\text{Mo}(\eta^3\text{-C}_3\text{H}_5)_4$, and $\text{Mo}_2(\eta^3\text{-C}_3\text{H}_5)_4$. Molybdenum loadings of 0.1–10 wt % were studied. LRS was also used to characterize dehydrated molybdenum oxide, under in situ conditions, prepared from $\text{Mo}_2(\eta^3\text{-C}_3\text{H}_5)_4$ at a loading of 6.4 wt % Mo. Fumed silica (Cab-O-Sil EH-5) and silica gels (Davison 952, Rhone-Poulenc X400LS, and Nishio Kogyo) were used as supports. Raman spectra were recorded either in ambient air following calcination or in an in situ cell under oxygen purge. For the hydrated, ambient samples, all precursors were found, by LRS, to form octahedrally coordinated surface polymolybdate species at Mo loadings above 0.4 wt %. No Raman evidence was found for the existence of isolated, surface molybdenum oxide tetrahedra. In situ Raman showed that the octahedrally coordinated, hydrated polymolybdate species could be reversibly transformed into an isolated structure upon dehydration. Four crystalline compounds were also observed: MoO_3 , CaMoO_4 , $\text{Na}_2\text{Mo}_2\text{O}_7$, and Na_2MoO_4 . The formation of these crystalline compounds depended upon the Mo loading, the method of preparation, and the presence of impurities on the support. UVDRS, without supplementary evidence, is shown to be ineffective in differentiating tetrahedrally and octahedrally coordinated molybdenum for the systems studied. The formation of the hydrated, octahedrally coordinated surface polymolybdate species is shown to be related to the aqueous chemistry of Mo^{6+} .

Introduction

Considerable research has been devoted to the synthesis and characterization of highly dispersed molybdenum oxide on silica.¹⁻⁷ Because molybdenum oxide interacts only weakly with silica, the

effectiveness of conventional impregnation with ammonium heptamolybdate (AHM; $(\text{NH}_4)_6\text{Mo}_7\text{O}_{24}\cdot 4\text{H}_2\text{O}$) in producing

(1) Rodrigo, L.; Marcinkowska, K.; Adnot, A.; Roberge, P. C.; Kaliaguine, S.; Stencel, J. M.; Makovsky, L. E.; Diehl, J. R. *J. Phys. Chem.* **1986**, *90*, 2690.

(2) Stencel, J. M.; Diehl, J. R.; D'Este, J. R.; Makovsky, L. E.; Rodrigo, L.; Marcinkowska, K.; Adnot, A.; Roberge, P. C.; Kaliaguine, S. *J. Phys. Chem.* **1986**, *90*, 4739.

(3) Marcinkowska, K.; Rodrigo, L.; Kaliaguine, S.; Roberge, P. C. *J. Mol. Catal.* **1985**, *33*, 189.

* To whom correspondence should be addressed.

[†] Current address: Union Carbide Corporation, P.O. Box 8361, South Charleston, WV 25303.

[‡] Current address: Sandia National Laboratories, Division 1845, Albuquerque, NM 87185.

samples with high dispersion or uniform structure has been limited. An alternate approach, based on the reaction between molybdenum compounds containing labile ligands, such as MoCl_5 , $\text{Mo}(\eta^3\text{-C}_3\text{H}_5)_4$, and $\text{Mo}_2(\eta^3\text{-C}_3\text{H}_5)_4$, and silica hydroxyl groups has been reported to produce uniform structures of isolated, tetrahedrally coordinated molybdenum oxide monomers, dimers, and cation pairs, even when the molybdenum oxide is examined under ambient conditions. Some controversy exists, however, as to the effectiveness of this technique.

Yermakov studied the reaction between $\text{Mo}(\eta^3\text{-C}_3\text{H}_5)_4$ and silica with infrared spectroscopy, volumetric ligand desorption, and hydrogen and oxygen uptake.⁸ The resulting surface species were proposed to consist of tetrahedrally coordinated molybdenum cations bonded to the silica network through two Si-O-Mo linkages and capped with zero, one, or two oxo oxygens ($\text{Mo}=\text{O}$) depending on the oxidation state: $(-\text{SiO})_2\text{Mo}^{2+}$, $(-\text{SiO})_2\text{Mo}^{4+}\text{O}$, or $(-\text{SiO})_2\text{Mo}^{6+}\text{O}_2$, respectively.

Candlin and Thomas⁹ and Iwasawa and co-workers⁶ supported both $\text{Mo}(\eta^3\text{-C}_3\text{H}_5)_4$ and $\text{Mo}_2(\eta^3\text{-C}_3\text{H}_5)_4$ on silica. In addition to measuring allyl ligand desorption and hydrogen and oxygen uptake, Iwasawa and co-workers characterized this system with X-ray photoelectron spectroscopy (XPS), electron spin resonance (ESR), ultraviolet-visible diffuse reflectance spectroscopy (UVDRS), photoluminescence, and extended X-ray absorption fine structure (EXAFS).^{6,10-13} Raman spectra of $\text{Mo}^{6+}/\text{SiO}_2$ could not be obtained.¹¹ The model developed by Iwasawa⁶ envisages isolated or paired bidentate MoO_4 tetrahedra or tetrahedral dimers joined by bridging oxygen, depending on the silica support and precursor. These species were reported to be stable under repeated oxidation and reduction cycles.

Rodrigo and co-workers¹⁻⁴ studied Mo/SiO_2 prepared from both $\text{Mo}(\eta^3\text{-C}_3\text{H}_5)_4$ and AHM and low-temperature oxygen chemisorption, XPS, LRS, and UVDRS. The 950-cm^{-1} Raman band, characteristic of highly dispersed molybdenum oxide, was found to be more intense for a 2% Mo/SiO_2 (expressed as percent Mo metal) sample prepared from $\text{Mo}(\eta^3\text{-C}_3\text{H}_5)_4$ than for a 2% Mo sample prepared from AHM, suggesting a higher dispersion for the former sample. Crystalline MoO_3 was found only on the sample prepared from AHM, although at Mo loadings above 1%, both series of samples were found to contain a silicomolybdic anion species, which has Raman shifts at 980, 667, 620, 245, 208, and 156 cm^{-1} , following hydration.^{1,2}

The ratio of oxygen chemisorbed at $-78\text{ }^\circ\text{C}$ to the oxygen removed by hydrogen reduction at $500\text{ }^\circ\text{C}$ was found to be relatively low for samples prepared from both precursors, for Mo loadings from 1 to 8%.¹ This was attributed to molybdenum oxide polymerization, resulting from its weak interaction with silica. Samples prepared from AHM and containing less than 1% Mo, on the other hand, were found to give unusually high ratios of chemisorbed oxygen per oxygen vacancy, suggesting that for these samples the impregnation technique led to polymeric molybdenum oxide outside of the pores. This hypothesis was also supported with XPS results, where samples prepared from AHM displayed a much higher surface Mo/Si ratio than samples prepared from $\text{Mo}(\eta^3\text{-C}_3\text{H}_5)_4$. When the outer surfaces of AHM-derived samples were ground off, the Mo/Si XPS ratio matched that of samples prepared from $\text{Mo}(\eta^3\text{-C}_3\text{H}_5)_4$, suggesting that even though surface segregation occurred for the former samples, the Mo distribution inside of the pores was similar for both series of catalysts. UVDRS

TABLE I: Calcium and Sodium Content of Silica Supports

silica	% Ca	% Na
Davison 952	0.053 ^a	0.017 ^b
Davison 952 (acid washed)	0.013 ^a	<0.017 ^c
Davison 952 (Na doped)	0.053 ^c	2.0 ^d
Davison 952 (Na doped)	0.053 ^c	0.5 ^d
Rhone-Poulenc X400LS	0.010 ^a	0.06 ^a
Nishio Kogyo	0.0085 ^a	0.0029 ^a
Cab-O-Sil EH-5	<0.0002 ^a	<0.0005 ^a

^a Determined by Galbraith Laboratories. ^b Determined by Bureau of Economic Geology, University of Texas. ^c Based on Davison 952 analysis. ^d As prepared. ^e Determined by supplier.

spectra of Mo/SiO_2 prepared from both precursors displayed bands considered to result from tetrahedrally coordinated Mo at 250–260 nm as well as from octahedrally coordinated Mo at 320–340 nm.^{3,4}

It was concluded¹ that Mo/SiO_2 samples prepared from $\text{Mo}(\eta^3\text{-C}_3\text{H}_5)_4$ had a higher dispersion than those prepared from AHM. This result was attributed to the higher accessibility of $\text{Mo}(\eta^3\text{-C}_3\text{H}_5)_4$ solutions to small pores rather than to the inherent chemical reactivity of the precursor with the support. Although $\text{Mo}(\eta^3\text{-C}_3\text{H}_5)_4$ led to higher dispersion of Mo^{6+} on silica than did AHM, it was clear that, for samples prepared from both precursors, the surface molybdate species formed were identical and all of the molybdenum oxide was not uniformly bonded to the silica surface.

Catalysts formed from the reaction of MoCl_5 with silica hydroxyl groups have been proposed by Che and co-workers to possess higher molybdenum oxide dispersion than catalysts prepared by impregnation from AHM.^{7,14,15} Monodispersed molybdenum oxide was characterized by a high percentage of oxygen-titratable Mo^{5+} at 77 K, as detected by ESR, and by the absence of the Mo^{5+} – Mo^{6+} intervalence bands at 1000 nm monitored with UVDRS. Fricke et al.,⁵ studying the same system and using the same techniques, concluded that the reaction of MoCl_5 with the support silanol groups results in dimeric surface $\text{Mo}_2\text{Cl}_{10}$ species which formed polymolybdate upon calcination. It has been pointed out that this discrepancy could be due to omission of a final ammonium hydroxide washing step in the preparation.⁷ Recent photoluminescence results for MoCl_5 -derived samples, however, have shown that molybdenum oxide polymerization is significant at Mo loadings below 0.37% Mo and above 0.07% Mo.¹⁶

Although a wide variety of supported metal oxides have been characterized with Raman spectroscopy,¹⁷ its use has been limited in studies of silica-supported catalysts prepared from MoCl_5 , $\text{Mo}(\eta^3\text{-C}_3\text{H}_5)_4$, and $\text{Mo}_2(\eta^3\text{-C}_3\text{H}_5)_4$,^{1,2,11} because of the low weight loadings (less than 0.05 monolayer) typically employed with these preparations. Recent advances in Raman spectroscopy instrumentation, however, now make this low weight loading region accessible to analysis. UVDRS has been widely used to determine supported molybdenum cation coordination.^{3,7,11,18-23} Raman spectroscopy is shown to provide a useful check on this technique. The work reported here applies LRS and UVDRS to Mo/SiO_2 samples prepared from a variety of precursors, $(\text{NH}_4)_6\text{Mo}_7\text{O}_{24}\cdot 4\text{H}_2\text{O}$, $\text{H}_2(\text{MoO}_3\text{C}_2\text{O}_4)\cdot 2\text{H}_2\text{O}$, MoCl_5 , $\text{Mo}(\eta^3\text{-C}_3\text{H}_5)_4$, and $\text{Mo}_2(\eta^3\text{-C}_3\text{H}_5)_4$, over a wide range of weight loadings, 0.1–10.0%

(4) Marcinkowska, K.; Rodrigo, L.; Kaliaguine, S.; Roberge, P. C. *J. Catal.* **1986**, *97*, 75.

(5) Fricke, R.; Hanke, W.; Ohlmann, G. *J. Catal.* **1983**, *79*, 1.

(6) Iwasawa, Y. *Advances in Catalysis*; Academic Press: New York, 1987; Vol. 35, p 265.

(7) Che, M.; Louis, C. *J. Phys. Chem.* **1987**, *91*, 2875.

(8) Yermakov, Y. I. *Catal. Rev.—Sci. Eng.* **1976**, *13*, 77.

(9) Candlin, J. P.; Thomas, H. *Adv. Chem. Ser.* **1974**, *No. 132*, 212.

(10) Iwasawa, Y.; Nakano, Y.; Ogasawara, S. *J. Chem. Soc., Faraday Trans. 1* **1978**, *74*, 2968.

(11) Iwasawa, Y.; Ogasawara, S. *J. Chem. Soc., Faraday Trans. 1* **1979**, *75*, 1465.

(12) Iwasawa, Y.; Sato, Y.; Kuroda, H. *J. Catal.* **1983**, *82*, 289.

(13) Iwasawa, Y.; Yamagishi, M. *J. Catal.* **1983**, *82*, 373.

(14) Che, M.; Louis, C.; Tatibouet, J. M. *Polyhedron* **1986**, *5*, 123.

(15) Louis, C.; Tatibouet, J. M.; Che, M. *J. Catal.* **1988**, *109*, 354.

(16) Anpo, M.; Kondo, M.; Coluccia, S.; Louis, C.; Che, M. *J. Am. Chem. Soc.* **1989**, *111*, 8791.

(17) Wachs, I. E.; Hardcastle, F. D.; Chan, S. S. *Spectroscopy (Eugene, Ore.)* **1986**, *1*, 30.

(18) Ashley, J. H.; Mitchell, P. C. H. *J. Chem. Soc. A* **1969**, 2730.

(19) Anmolov, C. N.; Krylov, O. V. *Kinet. Katal.* **1970**, *11*, 1028.

(20) Castellan, A.; Bart, J. C. J.; Vaghi, A.; Giordano, N. *J. Catal.* **1976**, *42*, 162.

(21) Gajardo, P.; Grange, P.; Delmon, B. *J. Phys. Chem.* **1979**, *83*, 1771.

(22) Jeziorowski, H.; Knozinger, H. *J. Phys. Chem.* **1979**, *83*, 1166.

(23) Fournier, J.; Louis, C.; Che, M.; Chaquin, P.; Masure, D. *J. Catal.* **1989**, *119*, 400.

Mo, on supports containing different amounts of impurities. This work demonstrates that, when hydrated, the oxidized surface molybdate structure is independent of the molybdenum content and precursor and that the formation of crystalline molybdenum compounds is determined by weight loading, preparation procedure, and support impurities. The in situ Raman results demonstrate that a different structure forms in the absence of adsorbed water. In companion papers we describe the hydrated, structures formed by molybdenum oxide on alumina²⁴ and magnesia²⁵ supports.

Experimental Section

Catalyst Preparation. Davison 952 (280 mg²/g), Cab-O-Sil EH-5 (380 m²/g), Rhone-Poulenc X400LS (400 m²/g), and Nishio Kogyo 30–60 mesh silica gel (567 m²/g) supports were used as received. The calcium and sodium contents of the silica supports, determined by Galbraith Laboratories, the University of Texas Bureau of Economic Geology, and respective silica suppliers, are given in Table I. The influence of sodium and calcium on supported molybdenum oxide was tested by washing Davison silica in dilute sulfuric acid (this sample is referred to as acid-washed silica) to remove these impurities²⁶ or by doping Davison silica with 0.5 or 2% Na from Na₂CO₃ (Fisher ACS grade; 0.01% Ca). Nishio Kogyo silica has been used to support Mo₂(η^3 -C₃H₅)₄ in a previous study.²⁷

MoCl₅ dissolved in diethyl ether was added to C₃H₅MgBr at –23 °C and allowed to react for 1 h to produce Mo(η^3 -C₃H₅)₄ in a procedure adapted from Wilke et al.²⁸ Mo₂(η^3 -C₃H₅)₄ was prepared from C₃H₅MgBr and Mo₂(CH₃CO₂)₄ after Candlin and Thomas.⁹ The structures of the allylmolybdenum compounds were verified by ¹H NMR. Approximately 6% of the molybdenum in the Mo(η^3 -C₃H₅)₄ solutions was present as Mo₂(η^3 -C₃H₅)₄. No Mo(η^3 -C₃H₅)₄ could be detected in the Mo₂(η^3 -C₃H₅)₄ solutions. Silica supports were calcined between 250 and 500 °C (depending on the amount of molybdenum allyl to be added) in dry air for 2 h, evacuated for 1 h, and then purged with argon for 1 h to remove adsorbed impurities, water, and excess hydroxyl groups. Pentane solutions of Mo(η^3 -C₃H₅)₄ or Mo₂(η^3 -C₃H₅)₄ were added to partially dehydroxylated silicas at 0 °C. Reactions were complete within 20 min. Excess pentane was filtered, and the samples were evacuated for 1 h. Samples were then ramped at 5 °C/min in pure hydrogen to 550 °C and held at this temperature for 1 h. After cooling, samples were calcined in pure oxygen at 500 °C for 1 h. The Mo content of samples prepared from Mo(η^3 -C₃H₅)₄, Mo₂(η^3 -C₃H₅)₄, and MoCl₅ was determined with atomic absorption (Varian AA-1475) after fusion with LiBO₂ at 1000 °C and dissolution in 1% HNO₃. Weight loadings obtained from allylic preparations ranged from 0.4 to 6.4% Mo.

Mo₂(CH₃CO₂)₄ was synthesized²⁹ from Mo(CO)₆ (Aldrich, 98%), glacial acetic acid (J. T. Baker, 99.9%), and acetic anhydride (Fisher, 98.8%). C₃H₅MgBr was prepared from C₃H₅Br (Aldrich, 99%) and Mg chips (Aldrich, 99.95+%). MoCl₅ (99.9+%) was supplied by Aldrich. Anhydrous pentane and diethyl ether solvents were dried for several days over sodium/benzophenone. Argon (Linde, 99.999%) and hydrogen (Linde, 99.999%) were further purified by passing through oxygen and water traps (Scientific Glass Engineering). Oxygen (Liquid Carbonic, 99.993%) was also passed through a water trap (SGE).

MoCl₅ vapor or MoCl₅ dissolved in cyclohexane was reacted with silica hydroxyl groups according to procedures adapted from

Che and Louis.⁷ The gas-phase synthesis was performed in a Pyrex U-tube. Silica, confined to one side of the U-tube by glass wool, was dehydroxylated at 250 °C. MoCl₅ was then introduced to the opposite side of the U-tube and evaporated at 200 °C into an argon stream passing through the silica. The liquid-phase reaction was performed in a cyclohexane solvent with a Soxhlet extractor. The dark brown solid resulting from both procedures consisted of adsorbed Mo₂Cl₁₀ dimers and molybdenum bonded to the silica through Si–O–Mo linkages.¹⁴ Upon exposure to air the solid became dark blue, indicative of the oxidation of Mo₂Cl₁₀ to the molybdenum oxide blues. The samples were washed with dilute, aqueous ammonia solutions. After this washing step only the molybdenum oxide chemically bound to the silica is proposed to remain.¹⁴ Alternately, for some samples, the excess polymolybdate was removed with pure methanol or diethyl ether. Preparation from MoCl₅ resulted in relatively low weight loadings, 0.1–1.3% Mo.

Silica pores were filled with aqueous H₂(MoO₃C₂O₄)·2H₂O (Climax Molybdenum Co.) solutions of pH 1.5 or pH 6. Samples prepared with 1.0 and 1.5% Mo were dried at 140 °C for 3 h followed by calcination at 500 °C for 3 h. Silica pores were filled with aqueous AHM (Alpha Products, 99.999%) at its natural pH of 5–6, dried at 140 °C for 4 h, and calcined at 500 °C for 3 h. Samples were prepared with 0.1–10% Mo. One 2% Mo/SiO₂ sample was prepared from aqueous AHM with the pH lowered to 1 by nitric acid. It was dried and calcined under the same conditions as were the others.

Laser-Raman Spectroscopy. Laser Raman spectra were obtained with a Spectra-Physics Ar⁺ laser (Model 2020-05) with the exciting line typically at 514.5 nm. The radiation intensity at the samples was varied from 40 to 200 mW. The scattered radiation was passed through a Spex Triplemate spectrometer (Model 1877) coupled to a Princeton Applied Research OMA III optical multichannel analyzer (Model 1463) with an intensified photodiode array cooled to –40 °C. Slit width ranged from 60 to 550 μ m. The spectra were recorded with an OMA III dedicated computer and software. The overall resolution was experimentally determined to be better than 2 cm^{–1}. Additional details concerning the Raman apparatus have previously been published.^{17,30}

For ambient Raman studies the samples were pressed into wafers and spun at 2000 rpm to avoid local heating or decomposition. Representative Mo/SiO₂ samples from each precursor were scanned several weeks after preparation with no further calcination than that listed above. The majority of the samples were further calcined overnight at 500–600 °C to minimize sample fluorescence. Their spectra were recorded immediately after removal from the oven. There were no changes in the shape and position of the molybdenum–oxygen vibrational signals after this second calcination, but the spectral quality was markedly improved due to a decrease in the fluorescent background.

For the in situ Raman studies a pressed wafer was placed into a stationary sample holder that was installed in an in situ cell. Details for this cell can be found elsewhere.³⁰ Spectra were recorded under ambient air, in flowing oxygen at 550 °C, and at 50 °C after cooling in flowing oxygen.

Ultraviolet-Visible Diffuse Reflectance Spectroscopy. UVDRS spectra were recorded with a Varian DMS 300 UV-vis spectrophotometer with a diffuse reflectance accessory. Samples were scanned after several months exposure to atmospheric moisture and immediately after calcination for 5 h at 500 °C. Samples were placed in quartz cuvettes and were scanned against a pure silica background. Reference samples [Na₂MoO₄ (Aldrich, 98+%), MoO₃ (Aldrich, 99.5+%), and (NH₄)₆Mo₇O₂₄·4H₂O (Alpha Products, 99.999%)] were scanned as received.

Raman Reference Compounds

Raman spectroscopy can be used to detect both crystalline compounds and surface species of supported molybdenum oxide. Although the crystalline compounds identified in this paper are

(24) Williams, C. C.; Ekerdt, J. G.; Jehng, J.-M.; Hardcastle, F. D.; Wachs, I. E. *J. Phys. Chem.*, following paper in this issue.

(25) Williams, C. C.; Roark, R. D.; Ekerdt, J. G.; Chen, C.-K.; Jehng, J.-M.; Hardcastle, F. D.; Wachs, I. E. Characterization of the Molybdenum Magnesia System. Manuscript in preparation.

(26) Spencer, N. *J. Catal.* **1988**, *109*, 187.

(27) Iwasawa, Y.; Ito, N.; Ishii, H.; Kuroda, H. *J. Chem. Soc., Chem. Commun.* **1985**, 827.

(28) Wilke, G.; Bogdanovic, B.; Hardt, P.; Heimbach, P.; Kerm, W.; Kroner, M.; Oberkirch, W.; Tanaka, K.; Steinrucke, E.; Walter, W.; Zimmermann, H. *Angew. Chem., Int. Ed. Engl.* **1966**, *5*, 151.

(29) Stephenson, T. A.; Bannister, E.; Wilkinson, G. *J. Chem. Soc.* **1964**, 2538.

(30) Machej, T.; Haber, J.; Turek, A. M.; Wachs, I. E. *J. Appl. Catal.* **1991**, *70*, 115.

located on the silica surface, they will not be referred to as surface molybdate species. This term is reserved for X-ray amorphous molybdates attached directly, however weakly, to the oxide support. Identification of supported crystalline compounds is relatively straightforward because their spectra are characterized by sharp peaks, are relatively insensitive to hydration effects, and are virtually identical with those of the corresponding unsupported compounds. Interpretation of Raman spectra of surface species is difficult because both octahedral (O_h) and tetrahedral (T_d) species have Raman bands for the Mo–O stretch in the 800–1000-cm⁻¹ region; therefore, it is not possible to discriminate structures solely on the basis of Mo–O stretching band position. Identification of the surface molybdate species is aided by studying the effects of hydration, relying (when possible) on complementary spectroscopic techniques, and by drawing analogies to the surface structures of other supported cations.

Fully oxidized molybdenum can be tetrahedrally or octahedrally coordinated. Tetrahedrally coordinated molecules possess four Raman-active fundamental vibrational modes: $\nu_1(A_1) + \nu_2(E) + \nu_3(F_2) + \nu_4(F_2)$. The most intense Raman band is usually due to the symmetric stretching mode ($\nu_1(A_1)$), and this mode typically appears at the highest frequency. A compilation of Raman shifts for T_d (and O_h) crystalline compounds can be found in ref 31. The symmetric stretching mode ranges from 869 cm⁻¹ for Pb–MoO₄³² to 1012 cm⁻¹ for Al₂(MoO₄)₃.³³ Octahedrally coordinated MoO₆ units possess only three Raman-active modes: $\nu_1(A_{1g}) + \nu_2(E_g) + \nu_3(F_{2g})$. More than three bands are commonly observed in octahedral Mo compounds because the MoO₆ units are usually geometrically distorted, leading to one short Mo–O bond which usually has the most intense Raman band and occurs at the highest frequency. This Raman band position is seen to range from 846 cm⁻¹ for γ -BiMoO₆³⁴ to 998 cm⁻¹ for MoO₃.³⁵ The frequency of the Mo–O stretching mode is dependent on the length of the Mo–O bond and not the structure (T_d versus O_h);³¹ therefore, band position alone is insufficient for structural assignments.

The appropriateness of crystalline compounds as reference structures for surface molybdate species must be questioned because of the overlap in the band position region for the Mo–O stretch of T_d and O_h Mo⁶⁺. Wachs and co-workers have shown that oxide-supported, hydrated V⁵⁺ responds to the local surface charge, with the structures formed being the same as the aqueous structures formed at the equivalent pH.^{36,37} Aqueous Mo⁶⁺ anions are expected, by analogy, to be appropriate reference compounds for the hydrated, surface molybdate species reported here. In aqueous solutions, molybdenum forms isolated, T_d MoO₄²⁻ above a pH of 7–8 and O_h clusters, such as Mo₇O₂₄⁶⁻ and Mo₈O₂₆⁴⁻, at lower pH, with heptamolybdate converting to octamolybdate at pH below ca. 2.2.^{38–40} The MoO₄²⁻ anion has Raman bands at 897 ($\nu_3(\text{Mo–O})$), 837 ($\nu_2(\text{Mo–O})$), and 317 cm⁻¹ ($\delta(\text{Mo–O})$), both of which coincide). The Mo₇O₂₄⁶⁻ anion has Raman bands at 943 ($\nu(\text{Mo–O})$), 903 ($\nu(\text{Mo–O})$), 362 ($\delta(\text{Mo–O})$), and 219 cm⁻¹ ($\delta(\text{Mo–O–Mo})$).³⁸ The β -Mo₈O₂₆⁴⁻ anion has Raman bands at 965 ($\nu(\text{Mo–O})$), 925 ($\nu(\text{Mo–O})$), 370 ($\delta(\text{Mo–O})$), and 230 cm⁻¹ ($\delta(\text{Mo–O–Mo})$).³⁸ The Mo–O stretching and bending modes and the Mo–O–Mo mode are used in assigning the structures of hydrated, oxide-supported Mo.

Several tetrahedral structures have been proposed for Mo prepared from Mo(η^3 -C₃H₅)₄, Mo₂(η^3 -C₃H₅)₄, and MoCl₅. Isolated¹⁰ and paired¹¹ MoO₄ tetrahedra should have Raman shifts

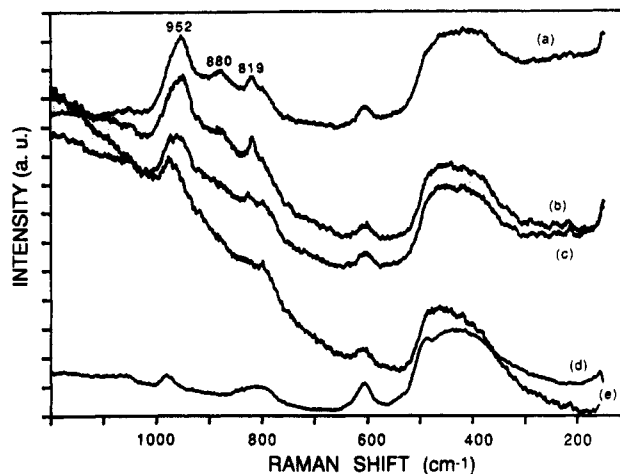


Figure 1. Raman spectra of hydrated Mo⁶⁺/SiO₂ prepared from (NH₄)₆Mo₇O₂₄·4H₂O and acid-washed Davison silica: (a) 0.8% Mo, (b) 0.6% Mo, (c) 0.4% Mo, (d) 0.2% Mo, and (e) pure SiO₂.

similar to the aqueous MoO₄²⁻ anion when hydrated. Iwasawa et al.²⁷ have proposed a T_d dimer pair formed from Mo₂(η^3 -C₃H₅)₄ over the Nishio Koygo support we have employed. Although many compounds contain tetrahedrally coordinated molybdenum, few are known to possess linked MoO₄ tetrahedra. The Mo₂O₇²⁻ anion, made up from two corner-sharing MoO₄ tetrahedra, is found in crystalline MgMo₂O₇⁴¹ and has been synthesized as a tetrabutylammonium salt.⁴² The Raman spectrum of this ion, obtained from molten K₂Mo₂O₇,⁴³ displays a Mo–O symmetric stretch at 927 cm⁻¹ and a Mo–O bend at 335 cm⁻¹. The antisymmetric stretching and symmetric bending modes of the Mo–O–Mo linkage were observed at 883 and 196 cm⁻¹, respectively. These linked tetrahedra are expected to serve as reference compounds for a surface molybdate dimer.

Results

Laser Raman Spectroscopy. Below we present the assignments of the Raman bands to facilitate the presentation of the results. A discussion of the polymolybdate assignment is provided in the next section. The CaMoO₄, Na₂MoO₄, Na₂Mo₂O₇, and MoO₃ assignments are made by direct comparison to published spectra.^{32,44–46} The following compounds have been identified with LRS on hydrated Mo⁶⁺/SiO₂: (1) polymolybdate characterized by broad features at 965–944, 880, 390–380, and 240–210 cm⁻¹; (2) MoO₃ with sharp peaks at 995, 819, 666, 417, 377, 338, 291, 248, 217, 198, and 160 cm⁻¹; (3) CaMoO₄ with sharp peaks at 878, 848, 794, 391, 325, and 206 cm⁻¹; (4) Na₂MoO₄ with peaks at 892, 808, 381, and 305 cm⁻¹; and (5) Na₂Mo₂O₇ with a peak at 938 cm⁻¹. The in situ Raman samples revealed that, when dehydrated, isolated Mo⁶⁺ species form with an intense band at 994–998 cm⁻¹.

Raman spectra of hydrated samples prepared from incipient wetness of acid-washed Davison silica with aqueous AHM are shown in Figure 1. As the Mo weight loading increases, the broad band initially observed near 970 cm⁻¹ (Figure 1c,d), which is a combination of the 944–965-cm⁻¹ Mo–O band and the 980-cm⁻¹ SiO₂ band, shifts to 952 cm⁻¹ (Figure 1a,b). A shoulder at 880 cm⁻¹ becomes observable at 0.6% Mo and is more pronounced at higher loadings (Figure 1a,b). As will be discussed below, these bands, as well as low-frequency bands observable only at higher Mo loadings, are due to a surface polymolybdate species. Broad features at 1065, 980, 800, 605, and 500–300 cm⁻¹ are due to the

(31) Hardcastle, F. D.; Wachs, I. E. *J. Raman Spectrosc.* **1990**, *21*, 683.

(32) Khanna, R. K.; Brower, W. S.; Guscott, B. R.; Lippincott, E. R. *J. Res. Natl. Bur. Stand., Sect. A* **1968**, *72*, 81.

(33) Zingg, D. S.; Makovsky, L. E.; Tischer, R. E.; Brown, F. R.; Hercules, D. M. *J. Phys. Chem.* **1980**, *84*, 2898.

(34) Teller, R. G.; Brazdil, J. R.; Grasselli, R. K.; Jorgensen, J. D. *Acta Crystallogr.* **1984**, *C40*, 2001.

(35) Giordano, N.; Bart, J. C. J.; Vaghi, A.; Castellan, A.; Martinotti, G. *J. Catal.* **1975**, *36*, 81.

(36) Eckert, H.; Wachs, I. E. *J. Phys. Chem.* **1989**, *93*, 6796.

(37) Deo, G.; Wachs, I. E. *J. Phys. Chem.* **1991**, *95*, 5889.

(38) Griffith, W. P.; Lesniak, P. J. *J. Chem. Soc. A* **1969**, 1066.

(39) Aveston, J.; Anacker, E. W.; Johnson, J. S. *Inorg. Chem.* **1969**, *3*, 735.

(40) Baes, C. F.; Mesmer, R. E. In *The Hydrolysis of Cations*; John Wiley & Sons: New York, 1976.

(41) Stadnicka, K.; Haber, J.; Kozłowski, R. *Acta Crystallogr.* **1977**, *B33*, 3859.

(42) Day, V. W.; Frerich, M. F.; Klemperer, W. G.; Shum, W. *J. Am. Chem. Soc.* **1977**, *99*, 6146.

(43) Becher, H. J. *J. Chem. Res. (M)* **1980**, 1053.

(44) Busey, R. H.; Keller, O. L., Jr. *J. Chem. Phys.* **1964**, *41*, 215.

(45) Becher, H. J. *Z. Anorg. Allg. Chem.* **1981**, *474*, 63.

(46) Py, M. A.; Schmid, Ph. E.; Vallin, J. T. *Nuovo Cimento* **1977**, *38B*, 271.

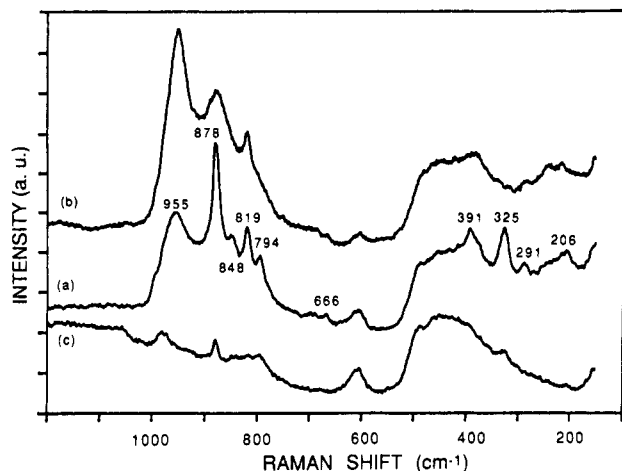


Figure 2. Raman spectra of hydrated $\text{Mo}^{6+}/\text{SiO}_2$ prepared from $(\text{NH}_4)_6\text{Mo}_7\text{O}_{24}\cdot 4\text{H}_2\text{O}$: (a) 2% Mo on Davison silica, (b) 2% Mo on acid-washed Davison silica, and (c) 0.1% Mo on Davison silica.

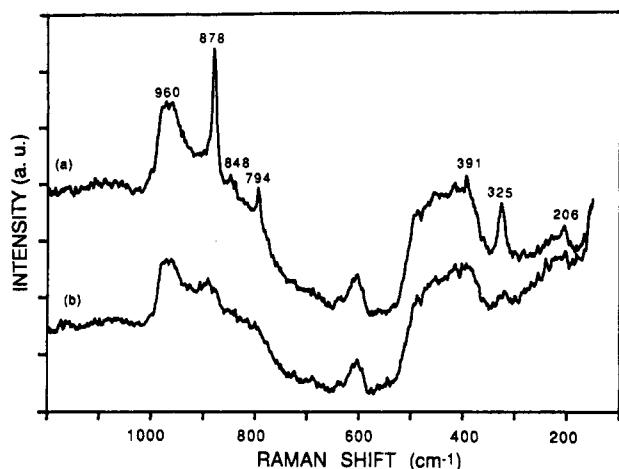


Figure 3. Raman spectra of hydrated 1.5% $\text{Mo}^{6+}/\text{SiO}_2$ prepared from $\text{H}_2(\text{MoO}_3\text{C}_2\text{O}_4)\cdot 2\text{H}_2\text{O}$: (a) at pH 6 and (b) at pH 1.5.

silica support (Figure 1e).⁴⁷ Beginning at 0.4% Mo, a sharp peak appears at 819 cm^{-1} , indicative of a trace amount of MoO_3 .⁴⁶

A similar series of samples were prepared by impregnation, with aqueous AHM, of as-received Davison 952 silica. The resulting Raman spectra contained bands due to polymolybdate and MoO_3 , as well as a series of sharp bands at 878, 848, 794, 391, 325, and 206 cm^{-1} , caused by CaMoO_4 .³² CaMoO_4 peaks are very intense in the Raman spectrum of 2% Mo/SiO_2 prepared by AHM impregnation of Davison 952 silica (Figure 2a). Peaks at 819, 666, and 291 cm^{-1} are due to MoO_3 . The Raman spectrum of 2% Mo/SiO_2 prepared by AHM impregnation of acid-washed Davison 952 silica (Figure 2b) shows a complete absence of the CaMoO_4 peaks. When Davison 952 silica was used to support AHM, CaMoO_4 could be detected at the lowest weight loading examined, 0.1% Mo (Figure 2c). CaMoO_4 and MoO_3 were observed when Rhone-Poulenc X400LS (0.010% Ca) was used to support 1% Mo from AHM. No CaMoO_4 was observed on 1% Mo/SiO_2 samples prepared from AHM on Cab-O-Sil EH-5 (<2 ppm Ca), although some MoO_3 was observed. All of the above-mentioned samples (containing more than 0.4% Mo) displayed the characteristic polymolybdate bands at 965–944 and 880 cm^{-1} . At higher loadings a broad polymolybdate band appeared at 240–210 cm^{-1} . In Figure 2 this band appears with MoO_3 and CaMoO_4 bands.

The formation of CaMoO_4 was dependent not only on the Ca content of the silica but also on the pH of the impregnation

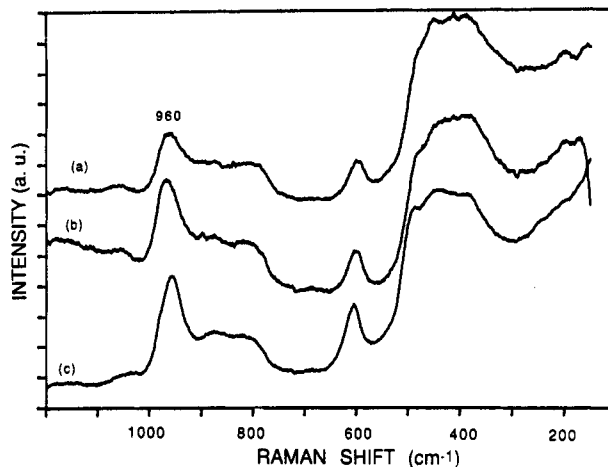


Figure 4. Raman spectra of hydrated $\text{Mo}^{6+}/\text{SiO}_2$: (a) 0.8% Mo prepared from $\text{Mo}(\eta^3\text{-C}_3\text{H}_5)_4$ and Davison silica, (b) 1.5% Mo prepared from $\text{Mo}_2(\eta^3\text{-C}_3\text{H}_5)_4$ and Davison silica, and (c) 1.3% Mo prepared from $\text{Mo}_2(\eta^3\text{-C}_3\text{H}_5)_4$ and Nishio silica.

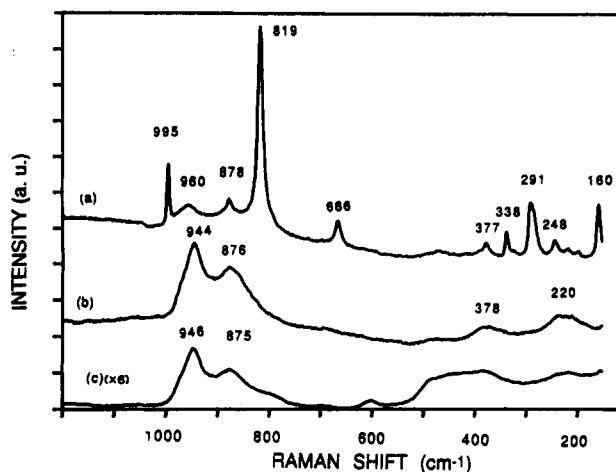


Figure 5. Raman spectra of hydrated $\text{Mo}^{6+}/\text{SiO}_2$: (a) 5.0% Mo prepared from $(\text{NH}_4)_6\text{Mo}_7\text{O}_{24}\cdot 4\text{H}_2\text{O}$ on Davison silica, (b) 6.4% Mo prepared from $\text{Mo}_2(\eta^3\text{-C}_3\text{H}_5)_4$ and acid-washed Davison silica, and (c) 1.1% Mo prepared from MoCl_5 and acid-washed Davison silica.

solution. As demonstrated in Figure 3, Raman spectra of Mo/SiO_2 prepared from $\text{H}_2(\text{MoO}_3\text{C}_2\text{O}_4)\cdot 2\text{H}_2\text{O}$ at pH 6 revealed CaMoO_4 , whereas minimal CaMoO_4 was observed on samples prepared at pH 1.5. Samples prepared at both pH 1.5 and pH 6 display the broad Raman band of polymolybdate at 965 cm^{-1} . The 1.5% Mo/SiO_2 sample prepared at pH 1.5 also displays the 880-cm^{-1} polymolybdate band. The 2% Mo/SiO_2 sample prepared from AHM and acid-washed silica at pH 1, below the point of zero surface charge (PZSC) of silica, displayed a spectrum identical with the 2% sample prepared at the natural pH (5–6) (Figure 2b).

The Raman spectra of hydrated Mo/SiO_2 prepared from $\text{Mo}(\eta^3\text{-C}_3\text{H}_5)_4$ on Davison silica (0.8% Mo) and from $\text{Mo}_2(\eta^3\text{-C}_3\text{H}_5)_4$ on both Davison (1.5% Mo) and Nishio (1.3% Mo) silicas are presented in Figure 4. Polymolybdate is again identified by the broad band at 960 cm^{-1} . The 880-cm^{-1} polymolybdate band is weak in these spectra, and no MoO_3 or CaMoO_4 was detected. Figure 5 presents the Raman spectra of hydrated 5% Mo/SiO_2 prepared by impregnation of Davison silica with AHM and of hydrated 6.4% Mo/SiO_2 prepared from $\text{Mo}_2(\eta^3\text{-C}_3\text{H}_5)_4$ and acid-washed Davison silica. No MoO_3 can be detected on the sample prepared from $\text{Mo}_2(\eta^3\text{-C}_3\text{H}_5)_4$, whereas the spectrum of the AHM-prepared sample was dominated by the sharp peaks of MoO_3 at 995, 819, 666, 417, 377, 338, 291, 248, 217, 198, and 160 cm^{-1} . Polymolybdate and CaMoO_4 are also detected on this sample by the bands at 955 and 878 cm^{-1} , respectively. Also shown in Figure 5c is the Raman spectrum of hydrated 1.1% Mo/SiO_2 prepared from MoCl_5 . This spectrum has the previously described

(47) Tallant, D. R.; Bunker, B. C.; Brinker, C. J.; Balfe, C. A. In *Better Ceramics Through Chemistry II (Proceedings of the Materials Research Society Symposium on Better Ceramics Through Chemistry)*; Brinker, C. J., Clark, D. E., Ulrich, D. R., Eds.; Materials Research Society: Pittsburgh, PA, 1986; pp 261–267.

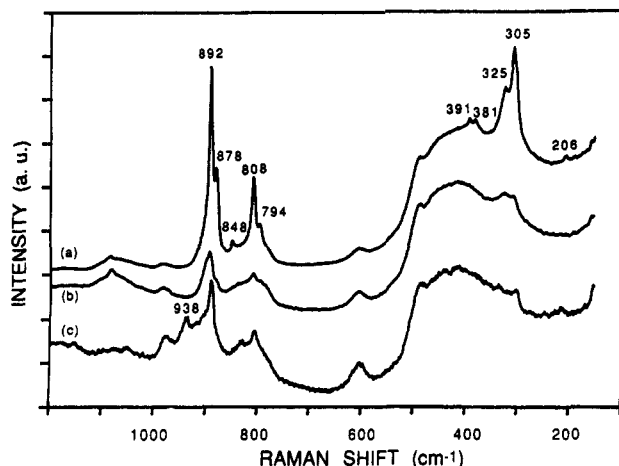


Figure 6. Raman spectra of hydrated $\text{Mo}^{6+}/\text{Na}/\text{SiO}_2$: (a) 1.0% Mo prepared from $(\text{NH}_4)_6\text{Mo}_7\text{O}_{24}\cdot 4\text{H}_2\text{O}$ and Davison silica doped with 2% Na, (b) 0.5% Mo prepared from $\text{Mo}_2(\eta^3\text{-C}_3\text{H}_5)_4$ and Davison silica doped with 2% Na, and (c) 1.0% Mo prepared from $\text{Mo}_2(\eta^3\text{-C}_3\text{H}_5)_4$ and Davison silica doped with 0.5% Na.

polymolybdate features, an intense band at 946 cm^{-1} , a Mo–O–Mo band at $240\text{--}220\text{ cm}^{-1}$, and a band at 390 cm^{-1} , that could be associated with the Mo–O bending mode. The bands at 220 and 380 cm^{-1} also appear for the 6.4% Mo/SiO₂ prepared from $\text{Mo}_2(\eta^3\text{-C}_3\text{H}_5)_4$ (Figure 5b). Approximately 12 MoCl_5 -derived $\text{Mo}^{6+}/\text{SiO}_2$ samples, containing 0.1–1.3% Mo, were examined. No Mo–O bands due to surface species other than polymolybdate could be detected.

Figure 6 presents the Raman spectra of hydrated 1% Mo/SiO₂ prepared from $(\text{NH}_4)_6\text{Mo}_7\text{O}_{24}$ and of 0.5% Mo/SiO₂ prepared from $\text{Mo}_2(\eta^3\text{-C}_3\text{H}_5)_4$ on Davison silica doped with 2% sodium. In addition to the CaMoO_4 peaks at 878, 848, 794, 391, 325, and 206 cm^{-1} , the 1% sample exhibits sharp peaks at 892, 808, 381, and 305 cm^{-1} caused by Na_2MoO_4 .⁴⁴ Inspection of the spectrum of the $\text{Mo}_2(\eta^3\text{-C}_3\text{H}_5)_4$ -derived 0.5% Mo/SiO₂ reveals CaMoO_4 and Na_2MoO_4 with the 878-cm^{-1} peak appearing as a shoulder on the 892-cm^{-1} peak. No polymolybdate band is seen at 960 cm^{-1} for these two samples. In addition to Na_2MoO_4 and $\text{Na}_2\text{Mo}_2\text{O}_7$, polymolybdate was detected on a 1% Mo sample prepared from $\text{Mo}_2(\eta^3\text{-C}_3\text{H}_5)_4$ and 0.5% Na/SiO₂.

The spectra of hydrated Mo/SiO₂ presented in Figures 1–6 were obtained within 1 h after calcination. When examined after 3-week exposure to atmospheric moisture, the Raman spectra of these samples were not changed.

Figure 7 presents the in situ Raman results for a 6.4 wt % Mo sample prepared from $\text{Mo}_2(\eta^3\text{-C}_3\text{H}_5)_4$ and acid-washed Davison silica. Spectra a (also shown in Figure 5b) and b of Figure 7 represent the hydrated state before and approximately 1 week after in situ treatment, respectively. The major features, when in the hydrated state, are the M–O stretching mode at $944\text{--}947\text{ cm}^{-1}$, the Mo–O–Mo deformation mode at 220 cm^{-1} , and bands at 876 and 380 cm^{-1} . The Mo–O–Mo deformation mode was absent and the Mo–O stretching mode shifted to $994\text{--}998\text{ cm}^{-1}$ when the sample was in the dehydrated state.

Ultraviolet–Visible Diffuse Reflectance Spectroscopy. Ultraviolet–visible diffuse reflectance spectra of three reference compounds are given in Figure 8. Na_2MoO_4 , possessing tetrahedrally coordinated molybdenum, displays a relatively narrow band at 265 nm and a broader shoulder at 230 nm. The broad absorption bands of compounds containing octahedrally coordinated molybdenum exhibit maxima at longer wavelengths, 325 nm for $(\text{NH}_4)_6\text{Mo}_7\text{O}_{24}\cdot 4\text{H}_2\text{O}$ and 330 nm for MoO_3 . A shoulder also appears on the spectra of both octahedral compounds near 230 nm.

UV spectra of $\text{Mo}^{6+}/\text{SiO}_2$ exposed to the atmosphere for 2 months after preparation from AHM display broad absorption curves whose maxima increase from 280 to 305 nm as Mo loading increases from 0.5 to 10% (Figure 9a–c). A broad shoulder at 360 nm appears in the spectrum of the 10% sample. After cal-

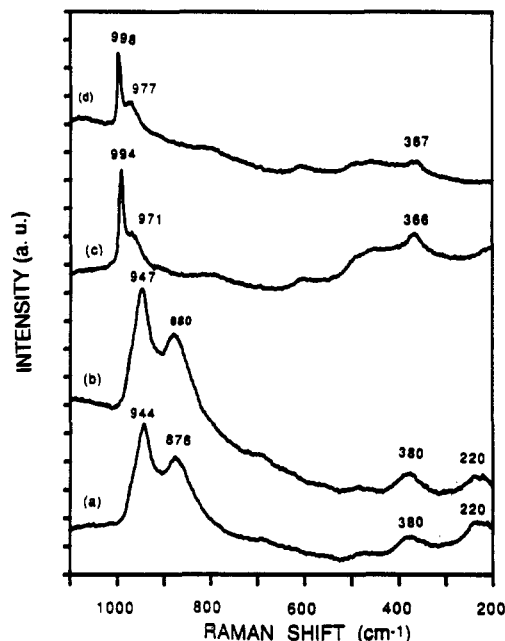


Figure 7. In situ Raman spectra for 6.4 wt % $\text{Mo}^{6+}/\text{SiO}_2$ prepared from $\text{Mo}_2(\eta^3\text{-C}_3\text{H}_5)_4$ and acid-washed Davison silica: (a) hydrated and at room temperature, (b) ca. 1 week after the in situ heating and reexposure of the sample to ambient air, (c) after heating to $550\text{ }^\circ\text{C}$ under oxygen purge and holding at $550\text{ }^\circ\text{C}$, and (d) after cooling to $50\text{ }^\circ\text{C}$ under oxygen purge.

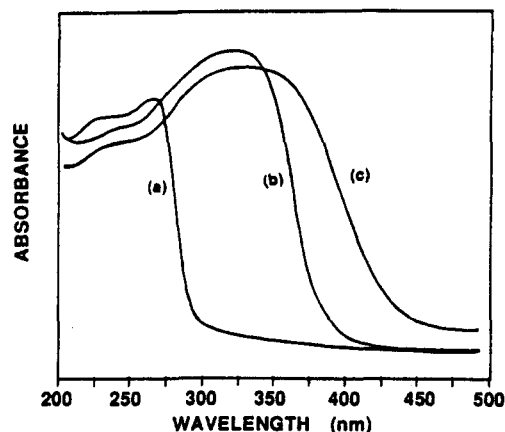


Figure 8. Ultraviolet–visible diffuse reflectance spectra of (a) Na_2MoO_4 , (b) $(\text{NH}_4)_6\text{Mo}_7\text{O}_{24}\cdot 4\text{H}_2\text{O}$, and (c) MoO_3 .

ination for 5 h at $500\text{ }^\circ\text{C}$, absorbance at longer wavelengths decreases and the 230-nm band becomes more pronounced (Figure 9d–f). The absorbance maxima now occur from 280 to 295 nm. Similar results were obtained with samples prepared from $\text{Mo}(\eta^3\text{-C}_3\text{H}_5)_4$, $\text{Mo}_2(\eta^3\text{-C}_3\text{H}_5)_4$, and MoCl_5 . Air-exposed samples (Figure 10a–c) absorb at higher wavelengths than freshly calcined samples. Tan-colored MoCl_5 -derived Mo/SiO₂, which was not calcined, absorbed from 225 to 475 nm (Figure 10d). The catalyst resulting from $\text{Mo}_2(\eta^3\text{-C}_3\text{H}_5)_4$ on Nishio silica was stored in a Schlenk tube and did not absorb as much at long wavelengths as did the other samples, which were stored in screw-top bottles (Figure 10a). Calcination at $500\text{ }^\circ\text{C}$ for 5 h reduced the absorbance at the higher wavelengths, and the spectra were nearly identical with those of calcined, impregnated catalysts (Figure 10e–h).

Discussion

Raman Data: Crystalline Compounds. Four crystalline molybdenum compounds (MoO_3 , CaMoO_4 , Na_2MoO_4 , and $\text{Na}_2\text{Mo}_2\text{O}_7$) are readily identified from the $\text{Mo}^{6+}/\text{SiO}_2$ Raman spectra in this study. Crystalline MoO_3 was only detected on samples prepared from AHM (Figures 1a–c, 2a,b, and 5a). MoO_3 was detected at a weight loading of 0.4% (0.09 Mo atom/nm²)

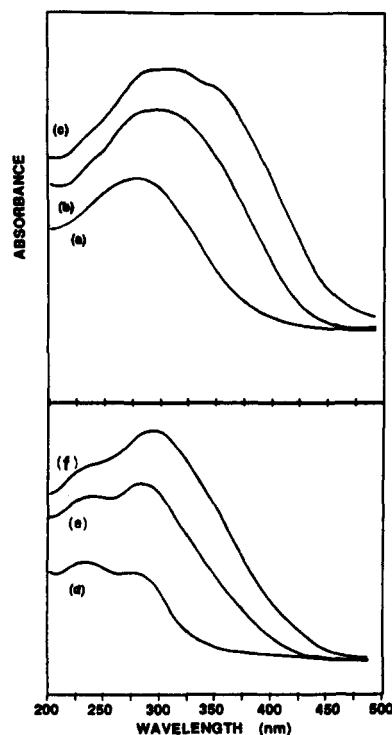


Figure 9. Ultraviolet-visible diffuse reflectance spectra of $\text{Mo}^{6+}/\text{SiO}_2$ prepared from $(\text{NH}_4)_6\text{Mo}_7\text{O}_{24}\cdot 4\text{H}_2\text{O}$ and Davison silica. (top) Scanned after 2 months of air exposure: (a) 0.5 wt % Mo, (b) 2 wt % Mo, and (c) 10 wt % Mo. (bottom) Scanned immediately after 5-h calcination at 500 °C: (d) 0.5 wt % Mo, (e) 2 wt % Mo, and (f) 10 wt % Mo.

on a sample prepared from incipient wetness of $(\text{NH}_4)_6\text{Mo}_7\text{O}_{24}$ on Davison silica and at a weight loading of 1% Mo (0.17 Mo atom/nm²) on Rhone-Poulenc and Cab-O-Sil, 1% being the lowest loading examined for these two supports.⁴⁸ Rodrigo et al.¹ and Thomas et al.⁴⁹ have detected silica-supported MoO_3 at slightly higher weight loadings, 2% (0.28 Mo atom/nm²) and 3.7% (0.46 Mo atom/nm²), respectively, for samples prepared from incipient wetness of $(\text{NH}_4)_6\text{Mo}_7\text{O}_{24}$. The absence of crystalline MoO_3 in the Raman spectra of samples prepared from MoCl_5 , $\text{H}_2(\text{MoO}_3\text{C}_2\text{O}_4)\cdot 2\text{H}_2\text{O}$, $\text{Mo}(\eta^3\text{-C}_3\text{H}_5)_4$, and $\text{Mo}_2(\eta^3\text{-C}_3\text{H}_5)_4$ at comparable weight loadings, 1.0–1.5 Mo (Figures 3, 4, and 5c), indicates that these precursors may bond to silica more readily than the heptamolybdate precursor and thereby maintain higher molybdenum oxide dispersion. Especially dramatic is the absence of MoO_3 at the highest Mo loading studied for the $\text{Mo}_2(\eta^3\text{-C}_3\text{H}_5)_4$ precursor, 6.4% Mo (Figure 5b), which corresponds to 1.3 Mo atoms/nm². A similar loading (5% Mo) prepared from AHM, an aqueous preparation, had less polymolybdate and a significant amount of MoO_3 (Figure 5a).

The inability of the heptamolybdate anion to penetrate the smallest support pores has been suggested by Rodrigo et al. to explain the formation of MoO_3 from AHM and not from $\text{Mo}(\eta^3\text{-C}_3\text{H}_5)_4$.¹ This well may have been the case for that study, in which the average silica support pore diameter was 19 Å. In our study, however, crystalline MoO_3 was found over Rhone-Poulenc, average pore diameter 110 Å, Davison 952, average pore diameter 140 Å, and nonporous Cab-O-Sil silica at 1% Mo, suggesting that factors other than pore dimensions control the supported structure. During impregnation with AHM solutions at pH levels above the PZSC of silica (pH ca. 4²⁵), the amount of negatively charged $\text{Mo}_7\text{O}_{24}^{6-}$ anions that can be adsorbed on the negatively charged silica surface is very limited. MoO_3 is likely formed from the anions remaining in the liquid-filled pores fol-

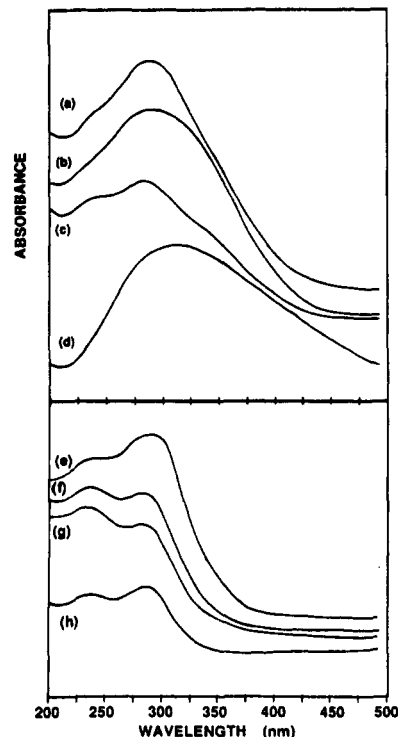


Figure 10. Ultraviolet-visible diffuse reflectance spectra of $\text{Mo}^{6+}/\text{SiO}_2$. (top) Air exposed for 2 months: (a) 1.0% Mo prepared from $\text{Mo}_2(\eta^3\text{-C}_3\text{H}_5)_4$ and Nishio silica, (b) 1.5% Mo prepared from $\text{Mo}_2(\eta^3\text{-C}_3\text{H}_5)_4$ and Davison silica, (c) 0.8% Mo prepared from $\text{Mo}(\eta^3\text{-C}_3\text{H}_5)_4$ and Davison silica, and (d) 0.33% Mo prepared from MoCl_5 and Davison silica. (bottom) Calcined at 500 °C for 5 h: (e) 1.0% Mo prepared from $\text{Mo}_2(\eta^3\text{-C}_3\text{H}_5)_4$ and Nishio silica, (f) 1.5% Mo prepared from $\text{Mo}_2(\eta^3\text{-C}_3\text{H}_5)_4$ and Davison silica, (g) 0.8% Mo prepared from $\text{Mo}(\eta^3\text{-C}_3\text{H}_5)_4$ and Davison silica, and (h) 0.33% Mo prepared from MoCl_5 and Davison silica.

lowing impregnation, during the drying and calcination steps. Higher polymolybdate loadings were formed from $\text{Mo}_2(\eta^3\text{-C}_3\text{H}_5)_4$, without MoO_3 formation, because the allylic complex does not adsorb as an anion. At the 2% Mo loadings used in this study, the amount of MoO_3 detected by LRS was the same for samples prepared at pH 1 and pH 5–6 from AHM. This is in contrast with a recent X-ray diffraction study of 8% Mo/SiO_2 which reported less MoO_3 formation for samples impregnated at pH 1, below the PZSC of silica, than for samples prepared above the PZSC.⁵⁰ The different sensitivities of LRS and XRD for MoO_3 may explain part of this discrepancy.

The sensitivity of LRS to crystalline compounds has been demonstrated by the scattering efficiencies of supported MoO_3 and polymolybdate phases. It has been estimated that crystalline MoO_3 is 17⁵¹ or 50–100⁴⁹ times more easily detected by LRS than surface molybdena. Some authors have concluded from temperature-programmed reduction (TPR)⁴⁹ and X-ray diffraction (XRD)⁵² that no more than 20% of the total molybdenum in Mo/SiO_2 catalysts exist as MoO_3 , for samples containing less than 5 Mo atoms/nm². Another XRD study reported that over 90% of the Mo was present as MoO_3 for $\text{Mo}^{6+}/\text{SiO}_2$ containing more than 7.5 Mo atoms/nm².⁵³ Assuming that the sensitivity of MoO_3 to polymolybdate is 17:1, our data suggest that at 5% Mo/SiO_2 approximately one-third of the Mo exists as MoO_3 . This amount increases to one-half for 10% Mo/SiO_2 . At 1.5% Mo/SiO_2 , only 5.3% was present as MoO_3 .

Certain Mo/SiO_2 samples prepared from aqueous routes contain another crystalline compound, CaMoO_4 . The sharp Raman peaks of CaMoO_4 can be seen to occur at 878, 848, 794,

(48) Raman is extremely sensitive to MoO_3 crystallites, and it may be present at trace levels when the Raman bands first become detectable.

(49) Thomas, R.; Mittelmeijer-Hazeleger, M. C.; Kerkhof, F. P. J. M.; Moulign, J. A.; Medema, J.; de Beer, V. H. J. In *Proceedings of the Climax 3rd International Conference on Chemistry and Uses of Molybdenum*; Climax Molybdenum Co.: Ann Arbor, MI, 1979; p 85.

(50) Ismail, H. M.; Theocharis, C. R.; Zaki, M. I. *J. Chem. Soc., Faraday Trans. 1* **1987**, *83*, 2835.

(51) Baltrus, J. P.; Makovsky, L. E.; Stencil, J. M.; Hercules, D. M. *Anal. Chem.* **1985**, *57*, 2500.

(52) Kakuta, N.; Tohji, K.; Udagawa, Y. *J. Phys. Chem.* **1988**, *92*, 2583.

(53) Ono, T.; Anpo, M.; Kubokawa, Y. *J. Phys. Chem.* **1986**, *90*, 4780.

391, 325, and 206 cm^{-1} in Figures 2a,c, 3a, and 5a. Similar peaks, quite weak in some cases, have appeared in Raman spectra of $\text{MoO}_3/\text{SiO}_2$ ^{1,2,49,52} and $\text{MoO}_3/\text{Al}_2\text{O}_3$ ⁵⁴⁻⁵⁷ but have not been identified as CaMoO_4 . CaMoO_4 was not formed when silicas with a calcium-free surface, Cab-O-Sil was acid-washed Davison (Figure 2b), were impregnated with $(\text{NH}_4)_6\text{Mo}_7\text{O}_{24}\cdot 4\text{H}_2\text{O}$. The high sensitivity of LRS toward CaMoO_4 is demonstrated in Figure 2a, in which the peaks due to CaMoO_4 , which is limited to 2.5% of the total molybdenum by the Ca content of the silica support, are twice as intense as the peaks due to polymolybdate, which contains at least 97.5% of the molybdenum in the sample.

Sodium has been reported to stabilize silica-supported molybdenum surface species prepared from $\text{Mo}_2(\eta^3\text{-C}_3\text{H}_5)_4$.⁶ The Mo-O bond length and XANES spectrum of pairs of $(\text{-O-})_2\text{Mo(=O)}_2$ species formed on silica doped with less than 0.5% Na were almost the same as those of K_2MoO_4 (Mo-O bond lengths: 1.78 and 1.74 Å).⁵⁸ Rather than stabilizing isolated or paired bidentate molybdenum oxide tetrahedra, our view is that sodium acts as a molybdenum scavenger, forming crystalline Na_2MoO_4 (Mo-O bond lengths in $\text{Na}_2\text{MoO}_4\cdot 2\text{H}_2\text{O}$: 1.752, 1.768, 1.781, and 1.788 Å;⁵⁹ Mo-O bond length for Na_2MoO_4 : 2.0 Å⁶⁰). Samples synthesized from $\text{Mo}_2(\eta^3\text{-C}_3\text{H}_5)_4$ and AHM supported on Davison silica doped with 2% Na contained only Na_2MoO_4 and CaMoO_4 . Na_2MoO_4 was not detected on undoped samples (Figures 1-5), even though the sodium content of unwashed Davison silica (0.017% Na) was higher than the calcium content of Rhone-Poulenc (0.01% Na) silica, which was sufficient calcium for CaMoO_4 formation.

Quantitative analysis revealed identical calcium content in untreated silica and Mo/SiO₂ samples, indicating that calcium was not introduced during impregnation. We propose that CaMoO_4 is formed primarily in the presence of water, during impregnation, and is therefore not detected on undoped samples prepared under anhydrous conditions from MoCl_5 , $\text{Mo}(\eta^3\text{-C}_3\text{H}_5)_4$, or $\text{Mo}_2(\eta^3\text{-C}_3\text{H}_5)_4$. Beltran et al.⁶¹ have determined that the aqueous $(\text{MoO}_2(\text{OH})_2(\text{C}_2\text{O}_4)_2)^{4-}$ ion decomposes to MoO_4^{2-} at pH > 4.25:



Heptamolybdate is also known to decompose to MoO_4^{2-} at pH > 5 in solutions used for impregnation.⁶²



During aqueous preparations with $(\text{NH}_4)_6\text{Mo}_7\text{O}_{24}$ solutions initially at pH 5-6 (Figure 2a) or $\text{H}_2(\text{MoO}_3\text{C}_2\text{O}_4)$ solutions initially at pH 6 (Figure 3a), MoO_4^{2-} precipitates with calcium dissolved from the support. Although the solubility of CaO increases with decreasing pH, CaMoO_4 does not precipitate when silica is impregnated with $\text{H}_2(\text{MoO}_3\text{C}_2\text{O}_4)$ solutions at pH 1.5 (Figure 3b) because the pH is too low to allow sufficient MoO_4^{2-} formation.

Na_2MoO_4 was not observed when undoped silicas were impregnated because it is soluble.⁶³ When Mo/SiO₂ was prepared from $(\text{NH}_4)_6\text{Mo}_7\text{O}_{24}$ on silica doped with 2% sodium, Na_2MoO_4 could crystallize as water was removed from the pores. Na_2MoO_4 could have formed from supporting $\text{Mo}_2(\eta^3\text{-C}_3\text{H}_5)_4$ on a 0.5 and

2.0% Na^+/SiO_2 surface (Figure 6b,c) by the migration of weakly held Mo species toward Na^+ cations during calcination.

The preceding results demonstrate that crystalline molybdenum compounds are readily formed from a variety of precursors, dopant levels, and support types. Crystalline compounds were formed more readily from aqueous than from anhydrous preparations. Because MoO_3 , CaMoO_4 , $\text{Na}_2\text{Mo}_2\text{O}_7$, and Na_2MoO_4 are catalytically less active than surface polymolybdates in some reactions, such as methanol oxidation,^{64,65} these crystalline compounds serve as molybdenum sinks and may therefore contribute to the lower activity of conventional, impregnated catalysts when compared at equivalent molybdenum loadings to catalysts prepared from $\text{Mo}(\eta^3\text{-C}_3\text{H}_5)_4$, $\text{Mo}_2(\eta^3\text{-C}_3\text{H}_5)_4$, and MoCl_5 . Furthermore, because CaMoO_4 and Na_2MoO_4 are readily detectable^{1,2,49,52,54-57} with LRS as tetrahedrally coordinated molybdenum, the presence of these supported crystalline compounds may lead to erroneous models featuring tetrahedrally coordinated surface compounds.

Raman Data: Hydrated Surface Molybdate Species. In addition to the crystalline compounds discussed above, Raman spectroscopy of hydrated samples revealed a surface molybdate species characterized by broad bands at 965-944, 880, 390-380, and 240-210 cm^{-1} . At least one of these bands, that at 965-944 cm^{-1} , occurred in the Raman spectrum of almost all (over 60) of the $\text{Mo}^{6+}/\text{SiO}_2$ samples examined. The exceptions were the previously discussed sodium-doped samples, where the molybdenum reacted with sodium and calcium on the support to form Na_2MoO_4 and CaMoO_4 , respectively, and the samples containing less than 0.4% Mo, where it was difficult to distinguish the 965- cm^{-1} Mo-O band from the 980- cm^{-1} silica mode. The Raman bands at 965-944, 880, 380, and 240-210 cm^{-1} are consistent with octahedrally coordinated polymolybdates, interacting weakly with the silica surface, similar in structure to the aqueous isopolymolybdate anions, $\text{Mo}_7\text{O}_{24}^{6-}$ and $\text{Mo}_8\text{O}_{26}^{4-}$. This conclusion is based on comparison with reference compounds and on weight loading and hydration effects for oxide-supported Mo^{6+} .²⁴

Several aqueous isopolymolybdate anions composed of edge-sharing MoO_6 octahedra display an intense Mo-O symmetric stretching vibration from 943 to 965 cm^{-1} ,^{38,66} corresponding to the most intense Raman peak of $\text{Mo}^{6+}/\text{SiO}_2$. Aqueous isopolymolybdate anions and $\text{Mo}^{6+}/\text{SiO}_2$ both exhibit a broad band at 210-240 cm^{-1} caused by the Mo-O-Mo deformation mode. This band appears clearly in the spectra of Figures 2a,b, 5c, 7a (5b), and 7b but is concealed at lower weight loadings by the silica background. A band at 360-370 cm^{-1} , corresponding to the Mo-O bending mode of $\text{Mo}_7\text{O}_{24}^{6-}$ or $\beta\text{-Mo}_8\text{O}_{26}^{4-}$, is very difficult to observe in the spectra of $\text{Mo}^{6+}/\text{SiO}_2$ because of the SiO_2 background. This mode may occur near 380 cm^{-1} in Figure 2b and is clearly visible in Figure 5b at 380 cm^{-1} .

In the next section we discuss the in situ Raman results. Spectra in Figure 7 show that the band at 944 cm^{-1} shifted to 998 cm^{-1} and the bands at 380 and 220 cm^{-1} were absent following dehydration at 550 °C. Similar shifts have been reported for Mo/TiO₂ upon dehydration in an in situ Raman cell.³⁰ After reexposure to ambient air, which causes rehydration, the Raman bands were seen at 947, 380, and 235-220 cm^{-1} (Figure 7), virtually identical with their initial frequencies. These in situ studies demonstrate that the $\text{Mo}^{6+}/\text{SiO}_2$ Raman bands reported herein for the hydrated samples (Figures 1-6) are associated with Mo^{6+} polycations that are solvated by adsorbed water. It is for this reason that the isopolymolybdate anions discussed above are the appropriate reference compounds for the $\text{Mo}^{6+}/\text{SiO}_2$ Raman bands measured under ambient conditions.

Aqueous Mo^{6+} forms discrete octahedral clusters at pH less than 6.2.^{38,39,62} The T_4 MoO_4^{2-} anion occurs above pH 7 or 8, and the equilibration between MoO_4^{2-} and O_h $\text{Mo}_7\text{O}_{24}^{6-}$ is a function of both the pH and concentration of the Mo^{6+} cation.^{39,40,62} Cab-O-Sil and acid-washed Davison silica used herein

(54) Brown, F. R.; Makovsky, L. E.; Rhee, K. H. *J. Catal.* **1977**, *50*, 162.

(55) Medema, J.; Van Stam, C.; De Beer, V. H. J.; Konings, A. J. A.; Koningsberger, D. C. *J. Catal.* **1978**, *53*, 386.

(56) Lopez Agudo, A.; Gil, F. J.; Calleja, J. M.; Fernandez, V. *J. Raman Spectrosc.* **1981**, *11*, 454.

(57) Dufresne, P.; Payen, E.; Grimblot, J.; Bonnelle, J. P. *J. Phys. Chem.* **1981**, *85*, 2344.

(58) Gatehouse, B. M.; Leverett, P. *J. Chem. Phys. A* **1969**, 849.

(59) Matsumoto, K.; Kobayashi, A.; Sasaki, Y. *Bull. Chem. Soc. Jpn.* **1975**, *48*, 1009.

(60) Lindqvist, I. *Acta Chem. Scand.* **1950**, *4*, 1066.

(61) Beltran, A.; Caturla, F.; Cervilla, A.; Beltran, J. *J. Inorg. Nucl. Chem.* **1981**, *43*, 3277.

(62) Luthra, N. P.; Cheng, W. C. *J. Catal.* **1987**, *107*, 154.

(63) The possibility that CaMoO_4 is a better Raman scatterer than Na_2MoO_4 cannot be excluded, leading to an inability to detect similar, low loadings of CaMoO_4 and Na_2MoO_4 .

(64) Williams, C. C.; Ekerdt, J. G. The Absence of Precursor Effects for Methanol Oxidation over Molybdenum Oxide Supported on Silica. *J. Catal.*, submitted for publication.

(65) Yang, T.-J.; Lunsford, J. H. *J. Catal.* **1987**, *103*, 55.

(66) Tytko, K. H.; Schonfeld, B. *Z. Naturforsch.* **1975**, *30B*, 471.

had a PZSC of 3.9 and 3.7, respectively, as determined²⁵ by the mass titration method.⁶⁷ Therefore, the surface of hydrated silica is equivalent to a low-pH solution. Furthermore, the PZSC decreased from 3.7 to 3.4 and 2.9 for Mo loadings of 0.1 and 0.5 wt %, respectively, on acid-washed Davison silica.²⁵ Solvated Mo⁶⁺ cations, on silica, are expected to respond to this low pH by forming O_h Mo⁶⁺ clusters.

The occurrence of the Mo–O symmetric stretching mode at frequencies ranging from 965 to 944 cm⁻¹, and the broadness of this band, suggest that a combination of Mo₇O₂₄⁶⁻ and Mo₈O₂₆⁴⁻ anion like species are most likely present on the surface. Although Mo₈O₂₆⁴⁻ is stable at pH values near the PZSC of silica, the occurrence of the surface molybdate ν (Mo–O) mode below that of the aqueous Mo₈O₂₆⁴⁻ anion at 965 cm⁻¹ and the stability of the Mo₇O₂₄⁶⁻ anion over a wide range of conditions^{38,39,68} suggest that Mo₇O₂₄⁶⁻ is the predominant species. Our model of a relatively weak interaction suggests that the surface molybdate clusters contain a discrete number of Mo cations (7–8) rather than a varying number, because discrete clusters are observed for solutions of molybdate anions.^{38,39,68}

The above interpretation is consistent with the literature, but the structural assignment is, in general, more specific. Jeziorowski et al. ascribed Raman bands at 956–970 and 884 cm⁻¹ to an analogue of a molybdenum polyanion chemically interacting with the silica support surface.⁶⁹ In a separate publication over Al₂O₃, this polymolybdate has been associated with either a two-dimensional structure consisting of MoO₆ octahedra linked together and anchored, via oxygen bridges, to the oxide support or a three-dimensional polyanion such as Mo₇O₂₄⁶⁻.⁷⁰ Rodrigo et al. observed only the broad band at 950 cm⁻¹ and suggested that it was indicative of a highly dispersed, surface molybdate but did not suggest a structure.¹ Similar Raman bands reported for Mo/SiO₂ at 950–980 and 855–880 cm⁻¹⁷¹ and at 950 and 880 cm⁻¹⁵² have been attributed to aggregated molybdenum species and to several types of octahedrally coordinated molybdates, respectively, but their identity is not well-defined. Thomas et al. have assigned the 960-cm⁻¹ band to an octahedral polymolybdate without offering a structure. The 860-cm⁻¹ band, in contrast, was assigned to a tetrahedral surface molybdate.⁴⁹

The intensity and position of the 880-cm⁻¹ band are different for the Raman spectra of the reference molybdate anions and the Mo/SiO₂ samples. At higher Mo loadings (Figures 1a, 2b, and 5b,c) the 950–960-cm⁻¹ polymolybdate band is accompanied by a band at 880 cm⁻¹, which is approximately 40% lower in intensity. This band is often unresolved from the background at lower Mo loadings (Figures 1c and 4a,b). Because the 880-cm⁻¹ band appears with the 944–960-cm⁻¹ band over a wide range of Mo loadings and on samples prepared from several precursors and silicas, it is proposed that this band is associated with the same surface molybdate species that causes the 944–960-cm⁻¹ band. The band at 880 cm⁻¹ is likely associated with the antisymmetric Mo–O–Mo stretch. A 880–850-cm⁻¹ Raman band has been observed on Mo/SiO₂ and Mo/Al₂O₃ and has been attributed to a low-frequency Mo–O stretching mode,²² a high-frequency Mo–O–Mo stretching mode,²² an Al–O–Mo stretching mode,⁷² and a surface tetrahedral molybdenum species.⁴⁹

The spectra for the highest Mo loading, having only surface molybdate, Figures 7a (5b) and 7b, clearly show the Mo–O stretch at 944–947 cm⁻¹. Aqueous Mo₇O₂₄⁶⁻ has Raman bands at 943, 898–903, and 840 cm⁻¹. Bands above 900 cm⁻¹ were associated with Mo–O stretches, and bands between 840–750 were assigned to the antisymmetric Mo–O–Mo stretch.³⁸ The diatomic approximation correlation demonstrates that changes in Mo–O bond

length (distortion of the octahedral MoO₆ unit) lead to changes in the position of the Raman band for the Mo–O stretch.³¹ This would cause the band at 944 cm⁻¹ to shift to higher frequencies if a second Mo–O stretching mode, associated with a Mo₇O₂₄ polyanion, shifts to 880 cm⁻¹. For this reason, since spectra a and b of Figure 7 are associated with a hydrated Mo₇O₂₄⁶⁻ cluster on silica, the band at 876 cm⁻¹ is unlikely to be associated with a Mo–O stretching mode.

The broad 880-cm⁻¹ band is not unlikely due to CaMoO₄ because it appears on samples (not shown) prepared anhydrously from Mo₂(η^3 -C₃H₅)₄ and Cab-O-Sil where the possibility from Ca contamination was avoided. Furthermore, the polymolybdate band at 880 cm⁻¹ is quite broad, whereas CaMoO₄ displays a very narrow Raman peak, even at very low concentrations (Figure 2c).

Raman Data: In Situ Surface Molybdate Species. The Raman spectra in Figure 7 show that a new structure reversibly formed upon dehydration. The dehydrated species displayed an intense Mo–O stretch at 994–998 cm⁻¹ and did not display the Mo–O–Mo bridging mode seen for the hydrated state. The absence of the Mo–O–Mo bridging mode suggests that Mo⁶⁺ transformed into isolated Mo⁶⁺ cations in the absence of water of hydration. Similar behavior was reported over TiO₂.³⁰ The polymolybdate band shifted to 1000 cm⁻¹ over TiO₂. Structure cannot be assigned solely on the basis of the Mo–O Raman position; independent spectroscopic information about the symmetry is also required. This independent information is required before a structure can be proposed for the isolated Mo⁶⁺ species that formed over silica upon dehydration.

Leyrer et al.⁷³ recently reported the spreading of MoO₃ on Al₂O₃ but were unable to obtain spreading over SiO₂. They examined spreading using dry O₂ and water-saturated O₂ and argued for a solid–solid wetting process rather than transport by gas-phase means or surface diffusion of a molybdenum hydrate species. Our experiments had as a starting point X-ray amorphous polymolybdate at a high loading (1.3 Mo/nm²) rather than MoO₃ crystallites. Spreading over SiO₂ may have occurred because different structures were present before the water of hydration was removed. An additional contributing factor in permitting the new structure to be observed in our work may have been the high loading of polymolybdate that was possible because the allylic synthesis route was used.

Ultraviolet–Visible Data. The common use of UVDRS to determine the local symmetry of supported molybdenum cations has recently been reviewed.²³ Crystalline molybdenum oxide compounds, for which Mo⁶⁺(T_d) and Mo⁶⁺(O_h) generally absorb at 260–290 and 300–330 nm,⁷⁴ respectively, and the aqueous MoO₄²⁻ and Mo₇O₂₄⁶⁻ anions, which absorb at 230–240 and 260–290 nm, respectively,^{22,75} have been used to model supported molybdenum oxide.²³ For oxide-supported Mo⁶⁺, early authors attributed the formation and growth of bands above 300 nm, observed with increasing molybdenum content, to a change in local molybdenum symmetry from tetrahedral to octahedral.^{11,18–21} Traditionally, absorption bands from 250 to 280 nm have been assigned to Mo(T_d) and bands from 300 to 330 nm were assigned to Mo(O_h).²³

Several results suggest that the local coordination of supported Mo⁶⁺ is not related to the UV absorption bands in the straightforward manner described above. Jeziorowski et al.,²² on the basis of an early study of molybdate solutions,⁷⁵ attributed bands between 250 and 290 nm to ligand charge-transfer transitions in the Mo–O–Mo groups, which are present in octahedral polymolybdate. Other authors have expressed the opinion that, for their respective cases, UV absorbances at wavelengths attributed to Mo(T_d), on the basis of reference compounds and the traditional interpretation given above, was actually due to octahedrally coordinated Mo⁶⁺.^{55,76}

(67) Schwarz, J. A.; Hoh, J. S. *J. Colloid Interface Sci.* **1989**, *130*, 157.

(68) Tytko, K. H.; Glemser, O. *Adv. Inorg. Chem. Radiochem.* **1976**, *19*, 239.

(69) Jeziorowski, H.; Knozinger, H.; Grange, P.; Gajardo, P. *J. Phys. Chem.* **1980**, *84*, 1825.

(70) Knozinger, H.; Jeziorowski, H. *J. Phys. Chem.* **1978**, *82*, 2002.

(71) Cheng, C. P.; Schrader, G. L. *J. Catal.* **1979**, *60*, 276.

(72) Kasztelan, S.; Payen, E.; Toulhoat, H.; Grimblot, J.; Bonelle, J. P. *Polyhedron* **1986**, *5*, 157.

(73) Leyrer, J.; Mey, D.; Knozinger, N. *J. Catal.* **1990**, *124*, 349.

(74) Che, M.; Figueras, F.; Forissier, M.; McAteer, J.; Perrin, M.; Portefaix, J. L.; Praliand, H. In *Proceedings of the 6th International Congress on Catalysis, London 1976*; The Chemical Society: London, 1977; Vol. 1, p 261.

(75) Bartecki, A.; Dembicka, D. *J. Inorg. Nucl. Chem.* **1967**, *29*, 2907.

The broad nature of electronic absorption bands, ill-characterized or differing reference compounds, and instrumentation differences have led to contradictory UV results. There is also significant overlap in the UV wavelengths attributed to Mo(T_d), 230²² to 295 nm,¹⁹ and to Mo(O_h), 270 to 330 nm.⁷⁷ Mo–O–Mo structures have been reported to absorb at 250–295²² and 320–340 nm.⁴

The relationship of spectral features to local molybdenum symmetry has recently been reexamined by Fournier et al.²³ The spectra of several well-characterized polyoxomolybdates revealed that the UV band position was relatively independent of Mo local symmetry and that the absorption increased in wavelength as the number of molybdenum octahedra in the anion was increased. Tsigdinos et al. have also correlated electronic absorption with molybdate aggregation rather than local molybdenum symmetry.⁷⁸

The literature suggests three possible interpretations of the UVDRS spectra (Figures 9 and 10): (1) the 230- and 280–295-nm peaks correspond to Mo(T_d) and Mo(O_h), respectively,⁷⁹ (2) the 280–295-nm peak is caused by Mo(T_d),¹¹ or (3) the 280–295-nm peak is due to Mo(O_h).⁷⁷ Because of possible instrumental differences and the wide variety of interpretations in the literature, based on both supported molybdenum phases and on reference compounds, the UVDRS data will be interpreted primarily on the basis of our reference compounds and Raman data. The first two interpretations lead to the conclusion that a large fraction of molybdenum oxide, even at Mo loadings as high as 10% (Figure 8a), is tetrahedrally coordinated, contrary to the Raman data. Furthermore, the first interpretation, suggesting that the 230-nm band is due to Mo(T_d), is not supported by the absorption of the Mo(T_d) reference compound Na_2MoO_4 at 265 nm. Only the third interpretation, that the 280–295-nm band is caused by Mo(O_h), is in agreement with the Raman data presented in this study. The band at 230 nm may also be associated with Mo(O_h), as it has been observed in the spectra of MoO_3 and $(\text{NH}_4)_6\text{Mo}_7\text{O}_{24}\cdot 4\text{H}_2\text{O}$ ^{23,80} (see also Figure 8). With increasing Mo content, the absorption maxima shift to higher wavelengths due to MoO_3 formation and, according to the conclusion of Fournier et al.,²³ increased polymolybdate aggregation. The slight amount of CaMoO_4 on the impregnated samples (<0.05% CaMoO_4) is assumed to make a negligible contribution to the UVDRS spectra. The calcination-induced change in UV spectra is due to loss of H_2O from polymolybdate anions and not a decrease in the amount of Mo(O_h).

Factors Controlling Surface Molybdate Structure. As mentioned in the Introduction, a large body of research is based on a $\text{Mo}^{6+}/\text{SiO}_2$ model incorporating tetrahedrally coordinated Mo cations.^{6–9,14–16} In the current study (as well as in published studies), no Raman evidence has been obtained for tetrahedrally coordinated molybdenum oxide on silica. Our work includes the allylic preparations prepared by Yermakov,⁸ Thomas and Candlin,⁹ and Iwasawa,⁶ and the MoCl_5 preparation described by Che and co-workers,^{7,14–16} and employed the same supports used by both Iwasawa and Che. We specifically examined weight loading ranges reported by Iwasawa (0.5–1 wt % Mo) and those reported by Che (0.1–1 wt % Mo). Furthermore, Raman spectra of Mo/ SiO_2 prepared by Che and co-workers using MoCl_5 are the same as those reported here.⁸¹ It is difficult to differentiate the octahedral polymolybdate symmetric stretch from the silica background at Mo loadings below 0.4% (0.09 Mo atom/nm²). Therefore, LRS cannot identify the surface structures present on silica below this loading in this study. Rodrigo et al.¹ concluded that for a 0.4% $\text{Mo}^{6+}/\text{SiO}_2$ sample (0.056 Mo atom/nm²) the

Mo–O stretch of the surface molybdate near 970 cm⁻¹ could be distinguished from the silica background, further decreasing the detectability limit of Mo(O_h).

The traditional UVDRS interpretation implies not only that Mo(T_d) exist at low Mo loadings but also that they remain even at high loadings.⁸² For example, Liu et al.⁸² have concluded that the majority of molybdenum oxide on silica is tetrahedrally coordinated even at 10% Mo. It may be possible that below 0.4% Mo some molybdenum oxide assumes tetrahedral coordination and is undetected by Raman spectroscopy, but certainly not 40–60% of the molybdenum on samples containing up to 10% Mo. Ultraviolet photoreduction studies with CO suggest that the structure of the molybdenum surface species is the same down to 0.07% Mo (0.011 Mo atom/nm²).⁸³ It has also been found that the methanol oxidation catalytic behavior attributed in the literature to isolated tetrahedrally coordinated molybdenum oxide¹⁵ could be due to impurities in the silica which lead to catalytically active molybdenum compounds.⁶⁴

The structures formed by hydrated molybdenum oxide overlayers on oxide carriers such as silica, alumina,²⁴ and magnesia²⁵ are governed by the acid–base properties of the supported and supporting phases; they appear not to be governed by the precursors. Not only does the PZSC of the oxide support determine the nature of the adsorbed molybdate species during aqueous impregnation, but also, as demonstrated in this paper and in the companion paper on $\text{Mo}^{6+}/\text{Al}_2\text{O}_3$,²⁴ the structure of calcined samples, after exposure to ambient conditions, is correlated with the PZSC of the support, in agreement with the conclusions of Leyrer et al.⁸⁴ Air-exposed samples rapidly become hydrated and contain surface hydroxyl groups as well as adsorbed water. The molybdate–support interaction for hydrated samples is therefore determined by the PZSC of the support. Because of the low PZSC of silica (ca. 4²⁵), molybdena assumes structures stable in an acidic aqueous environment, those of $\text{Mo}_7\text{O}_{24}^{6-}$ and $\text{Mo}_8\text{O}_{26}^{4-}$. For hydrated $\text{Mo}^{6+}/\text{Al}_2\text{O}_3$ (<1 Mo atom/nm²) samples,²⁴ molybdena assumes the MoO_4^{2-} structure which is stable under the aqueous basic conditions caused by the basic alumina (PZSC ca. 8²⁵) support. At higher molybdenum loadings on alumina (>1 Mo atom/nm²), the increase in acidity caused by Mo^{6+} ^{25,62,85} contributes to molybdate polymerization.

Conclusions

1. The structure of supported surface molybdates under ambient conditions (i.e., hydrated) is dependent on the inherent acid–base interactions with the support and not on the preparation procedure. The effect most dependent on precursor type is the formation, usually with impurities, of various crystalline molybdate phases.

2. Octahedrally coordinated polymolybdate, $\text{Mo}_7\text{O}_{24}^{6-}$ and $\text{Mo}_8\text{O}_{26}^{4-}$, was the only surface molybdate species observed on hydrated $\text{Mo}^{6+}/\text{SiO}_2$ samples prepared from $\text{H}_2(\text{MoO}_3\text{C}_2\text{O}_4)\cdot 2\text{H}_2\text{O}$, $\text{Mo}(\eta^3\text{-C}_3\text{H}_5)_4$, $\text{Mo}_2(\eta^3\text{-C}_3\text{H}_5)_4$, MoCl_5 , and $(\text{NH}_4)_6\text{Mo}_7\text{O}_{24}\cdot 4\text{H}_2\text{O}$. No Raman evidence was obtained for isolated tetrahedrally coordinated surface molybdates.

3. MoO_3 was formed, at trace levels, on samples prepared from $(\text{NH}_4)_6\text{Mo}_7\text{O}_{24}\cdot 4\text{H}_2\text{O}$ at molybdenum loadings as low as 0.4% (0.09 Mo atom/nm²). Significantly, MoO_3 was not formed at loadings up to 6.4% Mo on samples prepared from $\text{Mo}_2(\eta^3\text{-C}_3\text{H}_5)_4$.

4. CaMoO_4 forms when silicas, with calcium contents even as low as 0.01%, were impregnated with $\text{H}_2(\text{MoO}_3\text{C}_2\text{O}_4)\cdot 2\text{H}_2\text{O}$ and $(\text{NH}_4)_6\text{Mo}_7\text{O}_{24}\cdot 4\text{H}_2\text{O}$ at pH values above 5. Na_2MoO_4 , $\text{Na}_2\text{Mo}_2\text{O}_7$, and CaMoO_4 were preferentially formed on samples prepared from sodium-doped silica and $\text{Mo}_2(\eta^3\text{-C}_3\text{H}_5)_4$ and $(\text{NH}_4)_6\text{Mo}_7\text{O}_{24}\cdot 4\text{H}_2\text{O}$ due to strong acid–base reactions between

(76) Rodrigo, L.; Marcinkowska, K.; Roberge, P. C.; Kaliaguine, S. *J. Catal.* **1987**, *107*, 8.

(77) Praliand, H. *J. Less-Common Met.* **1977**, *54*, 387.

(78) Tsigdinos, G. A.; Chen, H. Y.; Streusand, B. *J. Ind. Eng. Chem. Prod. Res. Dev.* **1981**, *20*, 619.

(79) Rodrigo, L.; Marcinkowska, K.; Lafrance, C. P.; Roberge, P. C.; Kaliaguine, S. *Proc. 9th Iberoam. Symp. Catal.* **1984**, *675*.

(80) Giordano, N.; Bart, J. C. J.; Vaghi, A.; Castellan, A.; Martinotti, G. *J. Catal.* **1975**, *36*, 81.

(81) Wachs, I. E. Personal communication.

(82) Liu, T.; Forissier, M.; Coudurier, G.; Vadrine, J. C. *J. Chem. Soc., Faraday Trans. 1* **1989**, *85*, 1607.

(83) Williams, C. C.; Ekerdt, J. G. Transformation of Molybdenum Carbonyl Species formed by Ultraviolet Photoreduction of Silica-Supported Mo(VI) in Carbon Monoxide. *J. Phys. Chem.*, submitted for publication.

(84) Leyrer, J.; Vielhaber, B.; Zaki, M. I.; Zhuang, S.; Weitkamp, J.; Knozinger, H. *Mater. Chem. Phys.* **1985**, *13*, 301.

(85) Butz, T.; Vogdt, C.; Lurf, A.; Knozinger, H. *J. Catal.* **1989**, *116*, 31.

alkali-metal and molybdenum oxide.

5. In situ heating of 6.4 wt % Mo/SiO₂ destroyed the poly-molybdate clusters and led to the formation of a new Mo⁶⁺/SiO₂ structure in which the Mo⁶⁺ cations are isolated. The isolated Mo⁶⁺ species reformed a polymolybdate cluster upon rehydration of the surface.

6. Previously reported UVDRS bands attributed to tetrahedrally coordinated Mo were observed, but the assignment to Mo(*T_d*) is inconsistent with the LRS results which showed only

Mo(*O_h*) to be present.

Acknowledgment. This work was supported by the Robert A. Welch Foundation and the U.S. Department of Energy, Office of Basic Energy Sciences (C.C.W. and J.G.E), and by the Texaco Philanthropic Foundation (F.D.H.). We acknowledge Prof. Y. Iwasawa for supplying one of the silica supports.

Registry No. Molybdenum oxide, 1313-27-5; calcium, 7440-70-2; sodium, 7440-23-5.

A Raman and Ultraviolet Diffuse Reflectance Spectroscopic Investigation of Alumina-Supported Molybdenum Oxide

Clark C. Williams,[†] John G. Ekerdt,*

Department of Chemical Engineering, University of Texas at Austin, Austin, Texas 78712

Jih-Mirn Jehng, Franklin D. Hardcastle,[‡] and Israel E. Wachs

Zettlemoyer Center for Surface Studies, Departments of Chemical Engineering and Chemistry, Lehigh University, Bethlehem, Pennsylvania 18015 (Received: September 4, 1990; In Final Form: June 6, 1991)

Laser Raman spectroscopy and ultraviolet-visible diffuse reflectance spectroscopy were used to characterize alumina-supported molybdenum oxide prepared from Mo₂(η³-C₃H₅)₄, H₂(MoO₃C₂O₄)·2H₂O, and (NH₄)₆Mo₇O₂₄·4H₂O at loadings ranging from 0.67 to 13.3 wt % Mo. The structure of the calcined Mo⁶⁺/Al₂O₃, under ambient conditions, was found to be independent of the molybdenum precursor and the preparation pH. The hydrated surface molybdate structure was found to be governed by the inherent acid-base properties of the molybdena/alumina system and the molybdenum weight loading. At low Mo loadings (<1 Mo atom/nm²), isolated MoO₄ tetrahedra dominate although a low degree of polymerization was observed. At 2–2.5 Mo atoms/nm², the majority of the molybdenum was incorporated into octahedrally coordinated molybdenum polyanions. Crystalline MoO₃ was detected above monolayer coverage (5–6 Mo atoms/nm²).

Introduction

Conventional impregnation of alumina with aqueous molybdate salts has been claimed to result in catalysts with nonuniform dispersion and coordination.¹ Organometallic compounds, Mo(η³-C₃H₅)₄ and Mo₂(η³-C₃H₅)₄, as well as organic and inorganic salts, H₂(MoO₃C₂O₄)·2H₂O and (NH₄)₆Mo₇O₂₄·4H₂O (AHM), have recently been used under controlled conditions in an attempt to prepare highly dispersed and uniformly coordinated molybdenum oxide surface species on alumina. Iwasawa and co-workers have examined Mo/Al₂O₃ catalysts prepared from Mo(η³-C₃H₅)₄ and Mo₂(η³-C₃H₅)₄ with X-ray photoelectron spectroscopy (XPS), ultraviolet-visible diffuse reflectance spectroscopy (UVDRS), laser Raman spectroscopy (LRS), extended X-ray absorption fine structure (EXAFS), stoichiometric ligand removal, and hydrogen and oxygen uptake.^{2–4} The Raman spectrum of Mo(η³-C₃H₅)₄-derived Mo⁶⁺/Al₂O₃ displayed a Mo–O stretching band at 968 cm⁻¹ which was attributed to tetrahedrally coordinated Mo⁶⁺. The Mo⁶⁺/Al₂O₃ sample prepared from AHM displayed a Mo–O stretching band near 960 cm⁻¹ and was assigned to a pseudo-MoO₆ octahedral group.² They proposed that allylic precursors, after appropriate treatment, led to thermally stable, isolated or paired bidentate MoO₄ tetrahedra or tetrahedral dimers joined by bridging oxygen, depending on the alumina support and precursor. It was reported that the molybdenum in these compounds was uniformly coordinated and highly dispersed whereas in conventional catalysts, prepared from aqueous molybdenum salts, the molybdenum coordination number and degree of aggregation were variable.⁴ Rodrigo et al.,^{5–7} in contrast, obtained

nearly identical XPS, secondary ion mass spectroscopy (SIMS), and UVDRS results for catalysts prepared from AHM and Mo(η³-C₃H₅)₄. Although Mo(η³-C₃H₅)₄-derived samples at low weight loadings were more active in low-temperature oxygen chemisorption than impregnated samples, it was concluded from UVDRS data that these oxygen-consuming species were not isolated MoO₄ tetrahedra.

Wang and Hall developed a method to adsorb MoO₄²⁻ ions onto the alumina surface by maintaining the impregnation solution at pH 8–10.^{8,9} They concluded from LRS and UVDRS that molybdate anions adsorbed under these conditions remained isolated during drying and calcination, whereas conventional pore filling with the heptamolybdate anions present at lower pH values led to polymeric molybdate species. Kasztelan et al.,¹⁰ using a similar approach, have found that only 5% of the molybdenum adsorbed at low pH was removed by water washing after impregnation, whereas all of the molybdenum adsorbed at high pH could be removed, suggesting a limited interaction between MoO₄²⁻ anions and the negatively charged surface, which was above its

(1) Massoth, F. E. *Adv. Catal.* **1978**, *27*, 265.

(2) Iwasawa, Y.; Ogasawara, S. *J. Chem. Soc., Faraday Trans. 1* **1979**, *75*, 1465.

(3) Iwasawa, Y.; Sato, Y.; Kuroda, H. *J. Catal.* **1983**, *82*, 289.

(4) Iwasawa, Y. *Advances in Catalysis*; Academic Press: New York, 1987; Vol. 35, p 265.

(5) Rodrigo, L.; Marcinkowska, K.; Adnot, A.; Roberge, P. C.; Kaliaguine, S.; Stencel, J. M.; Makovsky, L. E.; Diehl, J. R. *J. Phys. Chem.* **1986**, *90*, 2690.

(6) Rodrigo, L.; Adnot, A.; Roberge, P. C.; Kaliaguine, S. *J. Catal.* **1987**, *105*, 175.

(7) Rodrigo, L.; Marcinkowska, K.; Lafrance, C. P.; Roberge, P. C.; Kaliaguine, S. *Proc. 9th Iberoam. Symp. Catal.* **1984**, 675.

(8) Wang, L.; Hall, W. K. *J. Catal.* **1980**, *66*, 251.

(9) Wang, L.; Hall, W. K. *J. Catal.* **1982**, *77*, 232.

(10) Kasztelan, S.; Grimblot, J.; Bonnelle, J. P.; Payen, E.; Toulhoat, H.; Jacquin, Y. *Appl. Catal.* **1983**, *7*, 91.

* To whom correspondence should be addressed.

[†] Current address: Union Carbide Corporation, P.O. Box 8361, South Charleston, WV 25303.

[‡] Current address: Sandia National Laboratory, Division 1845, Albuquerque, NM 87185.